

Unveiling Neutrino Mysteries with $\Delta(27)$ Symmetry.

Manash Dey^a Subhankar Roy^a

^a*Department of Physics, Gauhati University, India, 781014*

E-mail: manashdey@gauhati.ac.in, subhankar@gauhati.ac.in

ABSTRACT: An elegant model is proposed by extending the Standard Model using the $\Delta(27) \times Z_3 \times Z_{10}$ symmetry within the framework of the Type-I + Type-II seesaw mechanism. This model is particularly noteworthy for its ability to restrict the atmospheric mixing angle, θ_{23} , to specific values, and provides an explanation for the observed hierarchy of charged lepton masses. The neutrino mass matrix texture defined by three real parameters, predicts the three neutrino mass eigenvalues and the two Majorana phases. Furthermore, the model is tested against the experimental results of neutrino-less double beta ($0\nu\beta\beta$) decay and charged lepton flavour violation (cLFV) experiments.

Contents

1	Introduction	1
2	Theoretical Framework	3
3	Numerical Analysis	6
4	Neutrinoless Double Beta Decay	11
5	Charged Lepton Flavour Violation	15
6	Summary and Discussions	17
A	Appendix	23
A.1	The Pontecorvo-Maki-Nakagawa-Sakata matrix	23
A.2	$\Delta(27)$ group	24
A.3	Z_{10} group	25
A.4	Scalar Potential	25

1 Introduction

Over the past few decades, the Standard Model (SM) of particle physics, characterized by the gauge group $SU(2)_L \times U(1)_Y$, has gained widespread acceptance as a comprehensive theoretical framework that encompasses the fundamental particles, such as quarks and leptons and explains the fundamental interactions viz., the strong, weak, and electromagnetic interactions. Even though the SM is very successful in explaining a wide range of phenomena, but the theory is inefficient to explain neutrino mass origin, neutrino mass hierarchy, gravity, matter-antimatter asymmetry etc. Out of the many shortcomings, the inability to address the issues related to neutrino masses and mixing are the captivating problems in the realm of particle physics. The neutrinos [1] are massless in the framework of the SM. However, in the year 1957, Pontecorvo anticipated that neutrinos could change their flavour as they travel in space, a phenomenon known as neutrino oscillation [2]. The latter after experimental verification [3–5], in the recent past confirmed the fact that neutrinos are not massless. Therefore, it is apt to assert that the pursuit of finding answers to the missing pieces in the SM compels the model builders to go beyond the latter (BSM). In the context of the BSM theories, the neutrino mass matrix is an important quantity. The neutrino mass matrix, M_ν , originates from the Yukawa

Lagrangian (\mathcal{L}_Y), and it contains the information of masses and mixing. It encodes the information of all observational parameters which includes the solar mixing angle (θ_{12}), reactor mixing angle (θ_{13}), atmospheric mixing angle (θ_{23}), the neutrino mass eigenvalues (m_1, m_2, m_3), a Dirac CP-violating phase (δ), as well as two Majorana phases, namely α and β . The neutrino mass matrix is formulated within the framework of seesaw mechanism [6, 7].

There are many forms of seesaw mechanisms proposed in the literature. For example, the Type-I seesaw mechanism [8–12] is a simple extension of the SM, it introduces right-handed neutrinos (ν_R) to create both Majorana and Dirac mass terms, represented as $M_R(\bar{\nu}_R^c \nu_R)$ and $M_D(\bar{\nu}_L \nu_R)$ respectively. Here, the ν_L denotes the left-handed neutrino field from the SM doublet, M_D is the Dirac neutrino mass matrix and M_R is the right handed neutrino mass matrix. If one assumes that the scale of M_R is much larger than M_D , the neutrino mass matrix in Type-I seesaw is given by the expression,

$$-M_D.M_R^{-1}.M_D^T, \quad (1.1)$$

and the neutrino masses are observed to be of the order of around 10^{-2} eV. Therefore, the smallness of neutrino masses in this scenario can be attributed to the significant scale of M_R , which functions as a seesaw mechanism.

There is another type of seesaw mechanism known as Type-II seesaw [8, 12–15]. Here, one introduces a heavy $SU(2)_L$ scalar triplet, Δ , in the Higgs sector of the SM. The light Majorana neutrino mass term in this scenario, is given by $\sim y_\Delta(\bar{D}_{i_L} D_{i_L}^c) i\sigma_2 \Delta$. When $m_\Delta \gg v_h$, the neutral component of the scalar triplet acquires a non-zero vacuum expectation value (vev), v_Δ , it leads to a small Majorana neutrino mass: $m_\nu \sim y_\Delta v_\Delta$, where, $v_\Delta \sim v_h^2/m_\Delta^2$ and y_Δ is the corresponding coupling constant. Here, m_Δ represents the mass of the scalar triplet, and v_h signifies the SM Higgs vev ($v_h \sim 246$ GeV). This is to be underlined that one can generate the effective Majorana neutrino mass matrix in a framework where both Type-I and Type-II seesaw mechanisms may coexist. Such frameworks, most often, are referred to as the Type-I + Type-II seesaw mechanism [8, 16–19].

Though the neutrino mass matrix (M_ν) carries the information of all the observational parameters, but from the neutrino oscillation experiments, we can estimate only the mixing angles and δ . The neutrino oscillation experiments cannot give the exact values of the neutrino mass eigenvalues and the two Majorana phases. In this regard, if we can workout certain correlations among the neutrino mass matrix elements then we may address the problem of neutrino masses and mixing. A neutrino mass matrix exhibiting correlations are referred to as “textures”. In this connection, various phenomenological ideas have been proposed. These ideas include concepts like texture zeroes [20–22], μ - τ symmetry [23–26], $\mu - \tau$ mixed symmetry [27], $\mu - \tau$ reflection symmetry [28, 29], $\mu - \tau$ antisymmetry [26, 30], and more. These ideas are attributed to the neutrino mass matrix, M_ν , to place constraints on the

neutrino mass matrix elements and to draw significant phenomenological insights.

In this light, we shall try to formulate a similar texture starting from the seesaw mechanism, which predicts significantly on the oscillation parameters. The present work is interesting, as it shows a forbidden region for the atmospheric mixing angle, θ_{23} .

The structure of the work is as follows: In Section 2, we introduce the model, with a brief discussion of the discrete flavour symmetry, $\Delta(27)$ [31], which is employed in developing the neutrino mass matrix. We then delve into the field content, Lagrangian, and scalar potential of our model. In Section 3, we discuss the numerical analysis and key findings of our work. In Section 4 and Section 5, we test the predictability of the model in light of Neutrinoless Double Beta ($0\nu\beta\beta$) Decay and Charged Lepton Flavour Violation (cLFV) respectively. Finally, in Section 6, we highlight the summary and discussions of our work.

2 Theoretical Framework

We extend the SM gauge group with $\Delta(27)$ symmetry [31–36]. The discrete symmetry group $\Delta(27)$ has eleven irreducible representations, out of which there are one triplet (3), one anti-triplet ($\bar{3}$) and nine singlet ($1_{p,q}$) representations, where, $p, q = 0, 1, 2$. Unlike simple discrete symmetry groups such as A_4 [10, 37–39], which has got only two triplets (3) and three singlet ($1, 1', 1''$) representations, the presence of an additional anti-triplet ($\bar{3}$) representation within the framework of $\Delta(27)$ symmetry provides a greater flexibility for extracting important phenomenological insights.

We modify the SM field content by adding three singlet heavy right handed neutrinos viz., $\nu_{lR}(l=e,\mu,\tau)$, which under $\Delta(27)$ transform as $1_{00}, 1_{01}$ and 1_{02} . Two additional $\Delta(27)$ triplet scalar fields, χ and Δ are introduced, which individually transform as 1 and 3 under $SU(2)_L$. In addition to these, we consider five $SU(2)_L$ singlets η, κ, ξ, ζ and ϱ , transforming as $1_{01}, 1_{02}, 1_{00}, 1_{00}$ and 1_{00} under $\Delta(27)$ respectively. Two additional symmetries, Z_3 [40, 41] and Z_{10} [42–44] are introduced to restrict some undesirable and next to leading order terms in the Yukawa Lagrangian. We discuss the multiplication rules of $\Delta(27)$ and Z_{10} symmetries in the Appendix A.

The transformation of all the field contents under $SU(2)_L \times \Delta(27) \times Z_3 \times Z_{10}$ symmetry is highlighted in the Table (1).

The relevant Yukawa Lagrangian (\mathcal{L}_Y) of the model is shown below,

$$-\mathcal{L}_Y = \mathcal{L}_l + \mathcal{L}_\nu. \quad (2.1)$$

Where, \mathcal{L}_l and \mathcal{L}_ν , are for the charged leptons and neutrinos respectively, and they

Fields	\bar{D}_{l_L}	$D_{l_L}^c$	l_R	H	ν_{l_R}	χ	Δ	η	κ	ξ	ζ	ϱ
$SU(2)_L$	2	2	1	2	1	1	3	1	1	1	1	1
$\Delta(27)$	3	3	1_{0r}	1_{00}	1_{0r}	$\bar{3}$	3	1_{01}	1_{02}	1_{00}	1_{00}	1_{00}
Z_3	1	1	1	1	$(1, \omega^*, \omega^*)$	1	1	ω^*	ω^*	ω	ω	ω^*
Z_{10}	0	0	$(1,4,7)$	0	$(0,2,7)$	0	0	6	6	8	3	1

Table 1. The transformation properties of the field contents under $SU(2)_L \times \Delta(27) \times Z_3 \times Z_{10}$. Where, $r = 0, 1, 2$, $l = e, \mu, \tau$ and $\omega = e^{2\pi i/3}$.

are presented in the following manner,

$$\mathcal{L}_l = \frac{y_1}{\Lambda^{10}} (\bar{D}_{l_L} \chi) H e_R \varrho^9 + \frac{y_2}{\Lambda^7} (\bar{D}_{l_L} \chi) H \mu_R \varrho^6 + \frac{y_3}{\Lambda^4} (\bar{D}_{l_L} \chi) H \tau_R \varrho^3 + h.c. \quad (2.2)$$

and

$$\begin{aligned} \mathcal{L}_\nu = & \frac{y_e}{\Lambda} (\bar{D}_{l_L} \chi) \tilde{H} \nu_{e_R} + \frac{y_\mu}{\Lambda^2} (\bar{D}_{l_L} \chi) \tilde{H} \nu_{\mu_R} \xi + \frac{y_\tau}{\Lambda^2} (\bar{D}_{l_L} \chi) \tilde{H} \nu_{\tau_R} \zeta + \frac{1}{2} M_1 \overline{\nu_{e_R}^c} \nu_{e_R} + \frac{1}{2} \\ & y_s [\overline{\nu_{\mu_R}^c} \nu_{\tau_R} + \overline{\nu_{\tau_R}^c} \nu_{\mu_R}] \varrho + \frac{1}{2} y_{r_1} (\overline{\nu_{\mu_R}^c} \nu_{\mu_R}) \eta + \frac{1}{2} y_{r_2} (\overline{\nu_{\tau_R}^c} \nu_{\tau_R}) \kappa + y_\Delta (\bar{D}_{l_L} D_{l_L}^c) \tilde{\Delta} \\ & + h.c. \end{aligned} \quad (2.3)$$

Here, $\tilde{H} = i\sigma_2 H^*$, $\tilde{\Delta} = i\sigma_2 \Delta$ and Λ is the effective scale of the theory. After the scalars develop their respective vevs in the following way: $\langle \chi \rangle = v_\chi (1, 0, 0)$, $\langle H \rangle = v_h$, $\langle \Delta \rangle = v_\Delta (1, 1, 1)$, $\langle \eta \rangle = v_\eta$, $\langle \kappa \rangle = v_\kappa$, $\langle \varrho \rangle = v_\varrho$, $\langle \xi \rangle = v_\xi$ and $\langle \zeta \rangle = v_\zeta$, the charged leptons and the neutrinos acquire their masses. In this context, we wish to highlight that v_h , v_Δ and v_χ exhibit the following relationship,

$$v_\Delta v_\chi \sim \frac{2}{3} v_h^2. \quad (2.4)$$

This relation arises from the scalar potential, as discussed in the Appendix A. From this relation, we can estimate the vev, v_χ . By choosing v_Δ in the range of approximately $\sim 1\text{eV} - 1\text{ GeV}$ [14], and considering that $v_h = 246\text{ GeV}$, we find that v_χ lies in the range of approximately $\sim 4\text{ TeV} - 7 \times 10^6\text{ TeV}$.

Furthermore, it is important to mention that the Z_3 symmetry of \mathcal{L}_Y is broken by the vev of the scalar singlet ϱ . This breaking is important for the explanation of the charged lepton mass hierarchy [45–51].

From the \mathcal{L}_l , we extract the information of the charged lepton mass matrix (M_L), and it takes the form,

$$M_L = v_h v_\chi \begin{bmatrix} \frac{v_\varrho^9 y_1}{\Lambda^{10}} & 0 & 0 \\ 0 & \frac{v_\varrho^6 y_2}{\Lambda^7} & 0 \\ 0 & 0 & \frac{v_\varrho^3 y_3}{\Lambda^4} \end{bmatrix}. \quad (2.5)$$

The matrix M_L is a diagonal matrix, and it is observed that the charged lepton masses satisfy the following relation,

$$m_e : m_\mu : m_\tau \approx \lambda_m^6 y_1 : \lambda_m^3 y_2 : y_3, \quad (2.6)$$

where, $\lambda_m = v_\phi/\Lambda$. The above relation is in good agreement with the observed hierarchy of the charged lepton masses. The observed hierarchy is [52, 53],

$$m_e : m_\mu : m_\tau \approx 0.00028 : 0.05946 : 1. \quad (2.7)$$

To have a numerical understanding of the hierarchy predicted from our model, we may take the Yukawa couplings as, $y_1 \approx 0.1$, $y_2 \approx 1$ and $y_3 \approx 1$, and $\lambda_m \approx 0.38$. We find that, for these inputs, Eq. (2.6) is consistent with the observed hierarchy highlighted in Eq. (2.7).

To extract the information of the neutrino masses, we rewrite the \mathcal{L}_ν in the following way,

$$\mathcal{L}_\nu = \frac{1}{2} \bar{\nu}_L M_{II} \nu_L^c + \bar{\nu}_L M_D \nu_R + \frac{1}{2} \bar{\nu}_R^c M_R \nu_R + h.c. \quad (2.8)$$

where, M_D is the Dirac neutrino mass matrix, M_R is the right handed Majorana neutrino mass matrix and M_{II} is the mass matrix arising from Type-II seesaw mechanism. Although we have not written the flavour indices, it is understandable that M_D , M_R and M_{II} are 3×3 matrices in the flavour space. They are shown below,

$$M_D = \begin{bmatrix} \frac{v_h v_\chi y_e}{\Lambda} & 0 & 0 \\ 0 & \frac{v_h v_\chi v_\xi y_\mu}{\Lambda^2} & 0 \\ 0 & 0 & \frac{v_h v_\chi v_\zeta y_\tau}{\Lambda^2} \end{bmatrix}, \quad M_R = \begin{bmatrix} M_1 & 0 & 0 \\ 0 & y_{r_1} v_\eta & y_{s\varrho} \\ 0 & y_{s\varrho} & y_{r_2} v_\kappa \end{bmatrix}, \quad M_{II} = \frac{y_\Delta v_\Delta}{2} \begin{bmatrix} 2 & 1 & 1 \\ 1 & 2 & 1 \\ 1 & 1 & 2 \end{bmatrix}. \quad (2.9)$$

To understand the effective light neutrino masses, we can rewrite Eq. (2.8) in the following way,

$$\mathcal{L}_\nu = \frac{1}{2} \bar{n}^c M n + h.c., \quad (2.10)$$

with

$$n = \begin{bmatrix} \nu_L^c \\ \nu_R \end{bmatrix}, \quad (2.11)$$

and the 6×6 mass matrix,

$$M = \begin{bmatrix} M_{II} & M_D \\ M_D^T & M_R \end{bmatrix}. \quad (2.12)$$

The block diagonalisation of M gives the light effective neutrino mass matrix,

$$M_\nu = M_{II} - M_D.M_R^{-1}.M_D^T \quad (2.13)$$

Here, $M_I = -M_D.M_R^{-1}.M_D^T$ is the contribution arising from Type-I seesaw mechanism. The complex Majorana neutrino mass matrix (M_ν) in the Type-I+Type-II seesaw framework after simplification, takes the following form,

$$M_\nu = \begin{bmatrix} t - d & t/2 & t/2 \\ t/2 & t + a & \frac{t}{2} - c \\ t/2 & \frac{t}{2} - c & t + b \end{bmatrix}, \quad (2.14)$$

such that the *model parameters* viz., $y_e, y_\mu, y_\tau, y_{r_1}, y_{r_2}, y_s, y_\Delta, v_\chi, v_\Delta, v_h, v_\eta, v_\kappa, v_\rho, v_\xi, v_\zeta$ and M_1 are related to the *texture parameters* viz., a, b, c, d and t in the following way,

$$a = \frac{y_{r_2} v_\kappa v_h^2 v_\xi^2 v_\chi^2 y_\mu^2}{\Lambda^4 ((y_s v_\rho)^2 - y_{r_1} y_{r_2} v_\eta v_\kappa)}, \quad (2.15)$$

$$b = \frac{y_{r_1} v_\eta v_h^2 v_\xi^2 v_\chi^2 y_\tau^2}{\Lambda^4 ((y_s v_\rho)^2 - y_{r_1} y_{r_2} v_\eta v_\kappa)}, \quad (2.16)$$

$$c = \frac{y_s v_\rho v_h^2 v_\xi v_\zeta v_\chi^2 y_\mu y_\tau}{\Lambda^4 ((y_s v_\rho)^2 - y_{r_1} y_{r_2} v_\eta v_\kappa)}, \quad (2.17)$$

$$d = \frac{y_e^2 v_h^2 v_\chi^2}{\Lambda^2 M_1}, \quad (2.18)$$

$$t = y_\Delta v_\Delta. \quad (2.19)$$

The texture contains a correlation: $(M_\nu)_{12} = (M_\nu)_{13}$, and it is observed that the $\mu - \tau$ symmetry is broken as $a \neq b$.

Now, in order to draw predictions from a mass matrix, one needs to diagonalise it with the help of a diagonalising matrix. In the context of neutrino physics phenomenology, this diagonalising matrix is known as the Pontecorvo-Maki-Nakagawa-Sakata (PMNS) matrix, \tilde{U} [54]. A detailed discussion on the parametrisation of the PMNS matrix is shown in the Appendix A.

The diagonalising matrix \tilde{U} , constrains the M_ν such that all complex texture parameters viz., a, b, c, d and t can be expressed in terms three real texture parameters viz., $Re[d], Im[d]$ and $Re[t]$. Which means, these three independent real parameters can span M_ν , and all the predictions associated with it.

In the upcoming section, we shall discuss the numerical predictions of the model.

3 Numerical Analysis

We first conduct the analysis in the light of normal hierarchy of neutrino masses. The aim is to diagonalise M_ν with the matrix \tilde{U} , for which, we consider the entire 3σ

range [55, 56] of the mixing angles and δ as inputs. It is important to mention that, though we have given the 3σ range of the mixing angles as inputs, but the model restricts θ_{23} to take some specific values within the 3σ bound. We find that there is a forbidden region approximately $42.33^\circ < \theta_{23} < 47.50^\circ$ within the 3σ bound of θ_{23} , which is graphically represented in Fig.1. This is one of the highlighting features of this work.

In addition to the prediction of Majorana phases, the model predicts the three neutrino mass eigenvalues which are consistent with the experimental observables Δm_{21}^2 [55, 56], Δm_{31}^2 [55, 56] and $\sum m_i < 0.12\text{eV}$ [57]. The numerical values of these predictions are shown in Table 2. Furthermore, from the analysis, we also fetch the the numerical information of the free parameters, $Re[d]$, $Im[d]$ and $Re[t]$. The free parameters $Re[d]$, $Im[d]$ and $Re[t]$ are found to be in the ranges as shown in Table.3.

To understand the predictions graphically, we show the plots in Figs. 2(a), 2(b), 2(c) and 2(d). To visualize the free parameters, we highlight the Figs.2(e) and 2(f).

Prediction	Minimum	Maximum
m_1/eV	0.01719	0.0303
m_2/eV	0.01912	0.03155
m_3/eV	0.05249	0.05896
$\sum m_i/\text{eV}$	0.09	0.119
α	-89.93°	89.77°
β	-89.95°	89.97°

Table 2. Shows the numerical values of the predicted parameters in case of normal hierarchy.

Free parameters	Minimum	Maximum
$Re[d]/\text{eV}$	-0.030	0.042
$Im[d]/\text{eV}$	-0.042	0.040
$Re[t]/\text{eV}$	-0.017	0.018

Table 3. Highlights the maximum and minimum values of the free parameters in case of normal hierarchy.

For the inverted hierarchy of neutrino masses, we do the similar analysis. However, for this case, there is no constrained region for θ_{23} or the other two mixing angles. The numerical values of three neutrino mass eigenvalues and the two Majorana phases are presented in Table 4. Similar to the normal hierarchy, we observe that mass eigenvalues are consistent with the observables Δm_{21}^2 [55, 56], Δm_{31}^2 [55, 56] and $\sum m_i < 0.12\text{eV}$ [57]. We graphically represent the predicted parameters in Figs. 3(a), 3(b), 3(c) and 3(d).

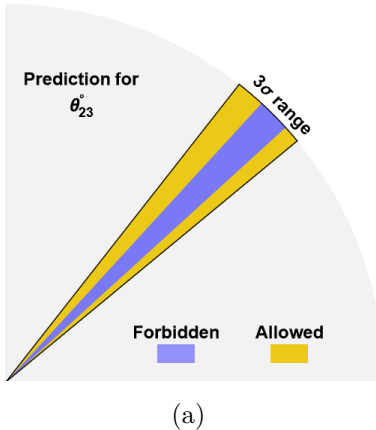


Figure 1. Constraints on θ_{23} set by our model in case of normal hierarchy.

The free parameters $Re[d]$, $Im[d]$ and $Re[t]$ in this case are found to be in the numerical ranges as shown in Table.5. We highlight the plots for free parameters in Figs. 3(e) and 3(f).

Prediction	Minimum	Maximum
m_1/eV	0.0491	0.0526
m_2/eV	0.0498	0.0533
m_3/eV	0.00014	0.0159
$\sum m_i/\text{eV}$	0.099	0.119
α	-89.95°	89.90°
β	-89.87°	89.88°

Table 4. Shows the numerical values of the predicted parameters in case of inverted hierarchy.

Free parameters	Minimum	Maximum
$Re[d]/\text{eV}$	-0.0589	0.0634
$Im[d]/\text{eV}$	-0.06216	0.06071
$Re[t]/\text{eV}$	-0.0126	0.0140

Table 5. Highlights the maximum and minimum values of the free parameters in case of inverted hierarchy.

Information of the Model Parameters

It is evident from Eq.(2.15)- Eq.(2.19), that the model parameters can be expressed in terms of the texture parameters. However, the present model has sixteen model parameters, and we can only extract information about certain combinations of these

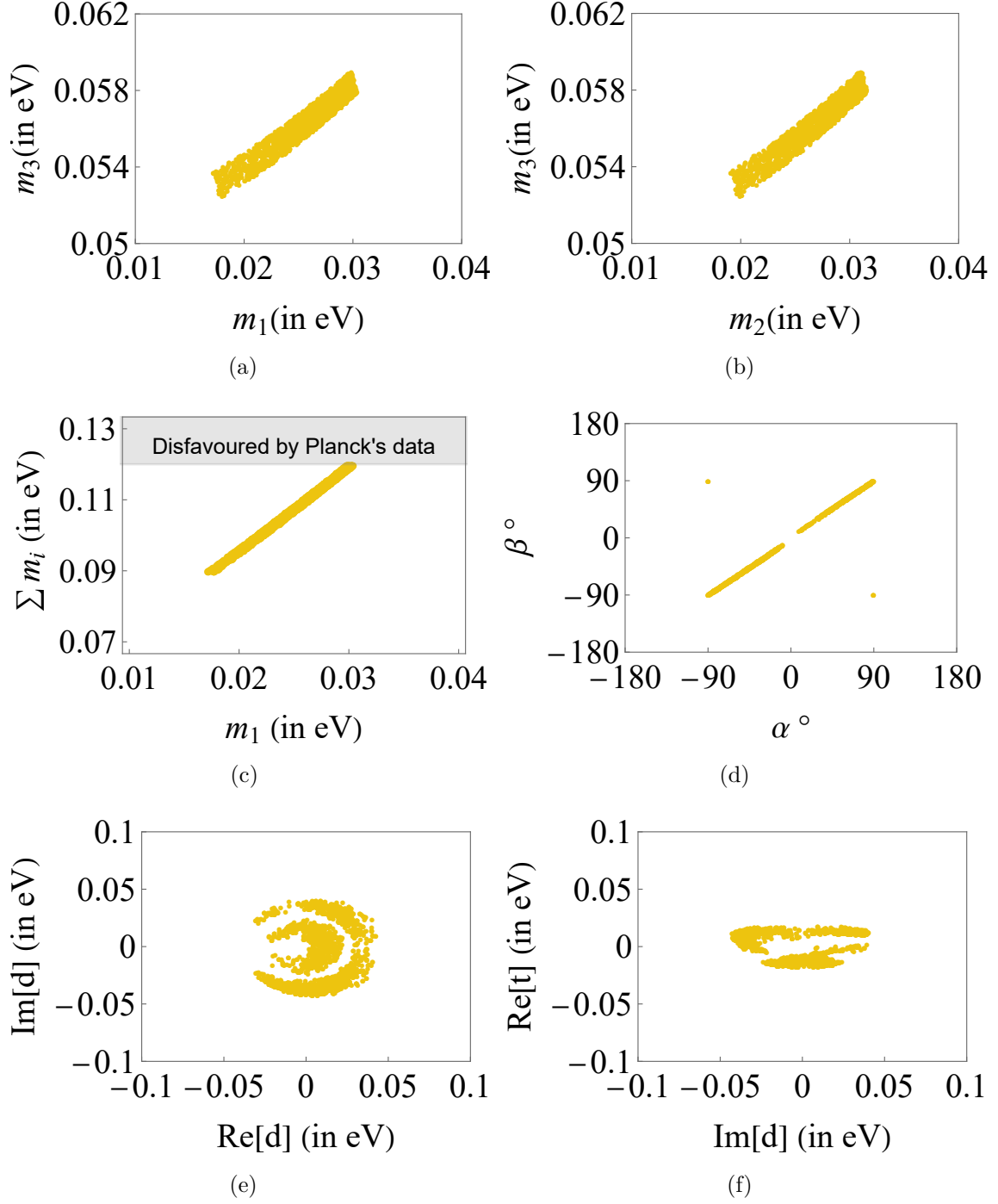


Figure 2. Represents the correlation plots for the mass eigenvalues, sum of the neutrino mass eigenvalues, Majorana phases and the free parameters in case normal hierarchy of neutrino masses.

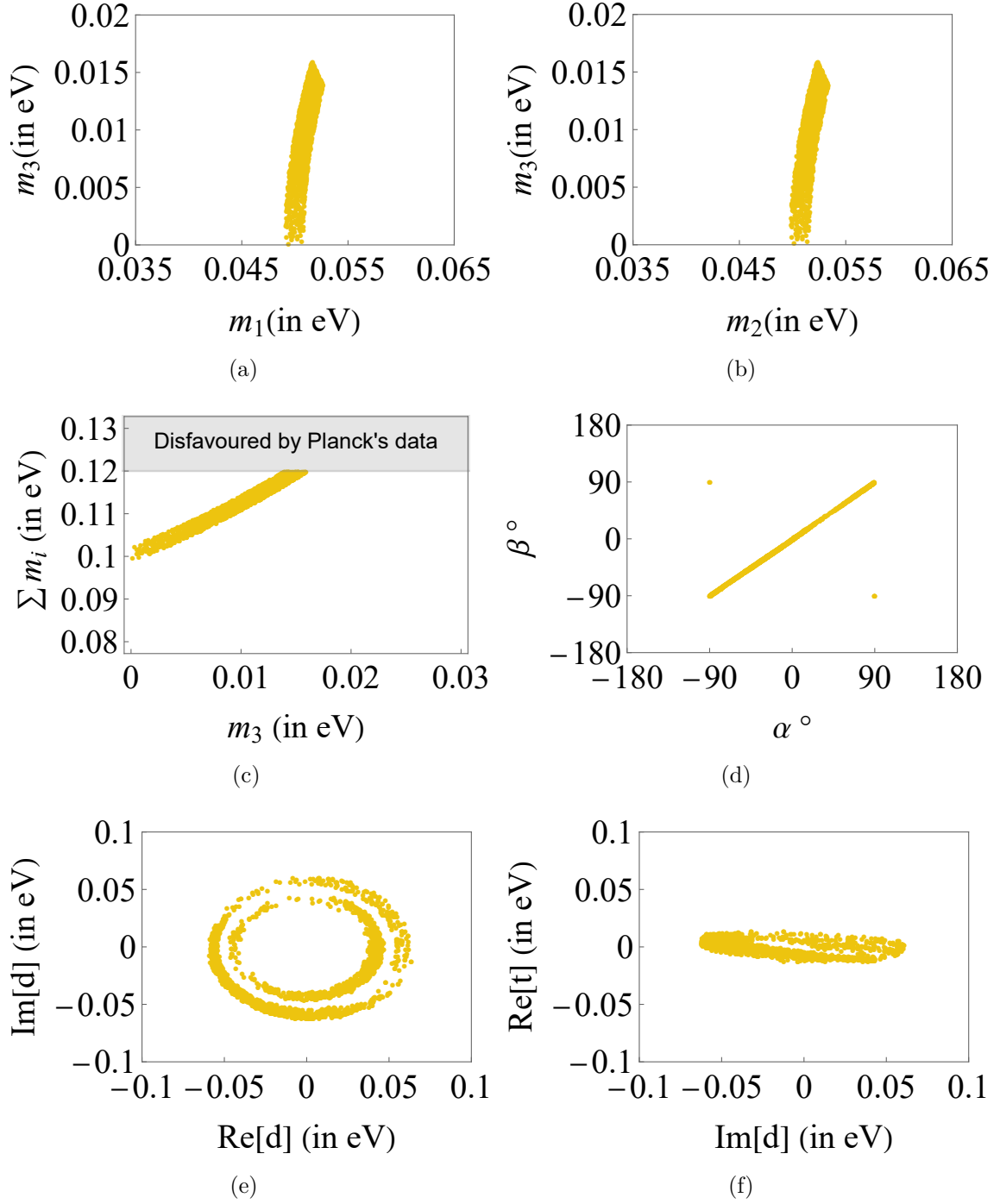


Figure 3. The correlation plots for the mass eigenvalues, sum of the three neutrino mass eigenvalues, Majorana phases and the free parameters in case of inverted hierarchy of neutrino masses.

parameters. In this regard, we highlight the combinations: C_1, C_2, C_3, C_4 and C_5 as shown below,

$$C_1 = \frac{v_h v_\chi y_e}{\Lambda \sqrt{M_1}}, \quad C_2 = \frac{v_h v_\chi v_\xi y_\mu \sqrt{y_{r_2} v_\kappa}}{\Lambda^2 y_s \varrho}, \quad C_3 = \frac{v_h v_\zeta v_\chi y_\tau}{\Lambda^2 \sqrt{y_{r_2} v_\kappa}},$$

$$C_4 = \frac{y_{r_1} v_\eta y_{r_2} v_\kappa}{y_s^2 \varrho^2}, \quad C_5 = v_\Delta y_\Delta. \quad (3.1)$$

It is needless to mention that these combinations are the functions of the free parameters $Re[d]$, $Im[d]$ and $Re[t]$. Therefore, we can extract numerical information about these model parameter combinations for both hierarchies of neutrino masses. The numerical values of these combinations are crucial for calculating the branching ratio of $\mu \rightarrow e\gamma$ decay, with C_5 being particularly significant for this calculation. We show the numerical values of C_1, C_2, C_3, C_4 and C_5 in Table 6 and Table 7. For a graphical representation of these combinations, the plots are highlighted in Figs.4(a)-4(h) for the normal hierarchy and Figs.5(a)-5(h) for the inverted hierarchy.

Parameter	Minimum	Maximum
$ C_1 /\text{eV}^{\frac{1}{2}}$	0.052	0.216
$ C_2 /\text{eV}^{\frac{1}{2}}$	0.036	0.812
$ C_3 /\text{eV}^{\frac{1}{2}}$	0.080	0.742
$ C_4 $	0.011	16.530
$ C_5 /\text{eV}$	0.006	0.0191
$Arg[C_1]/^\circ$	-79.921	82.001
$Arg[C_2]/^\circ$	-179.974	179.970
$Arg[C_3]/^\circ$	-175.861	178.480
$Arg[C_4]/^\circ$	-177.820	178.874
$Arg[C_5]/^\circ$	-179.944	179.863

Table 6. Represents the maximum and minimum values of the model parameters for normal hierarchy of neutrino masses.

The model is now equipped with the all the numerical informations necessary to study the $0\nu\beta\beta$ decay and cLFV.

4 Neutrinoless Double Beta Decay

The Model adheres to the Majorana nature of the neutrinos, therefore, it is pertinent to discuss the effective Majorana neutrino mass, $m_{\beta\beta}$. The $m_{\beta\beta}$ is an important observable parameter involved in the half life ($T_{1/2}$) of $0\nu\beta\beta$ decay [58–66]. The expression for $m_{\beta\beta}$, is given by,

$$m_{\beta\beta} = |U_{ei}^2 m_i|, \quad \text{where, } i = 1, 2, 3. \quad (4.1)$$

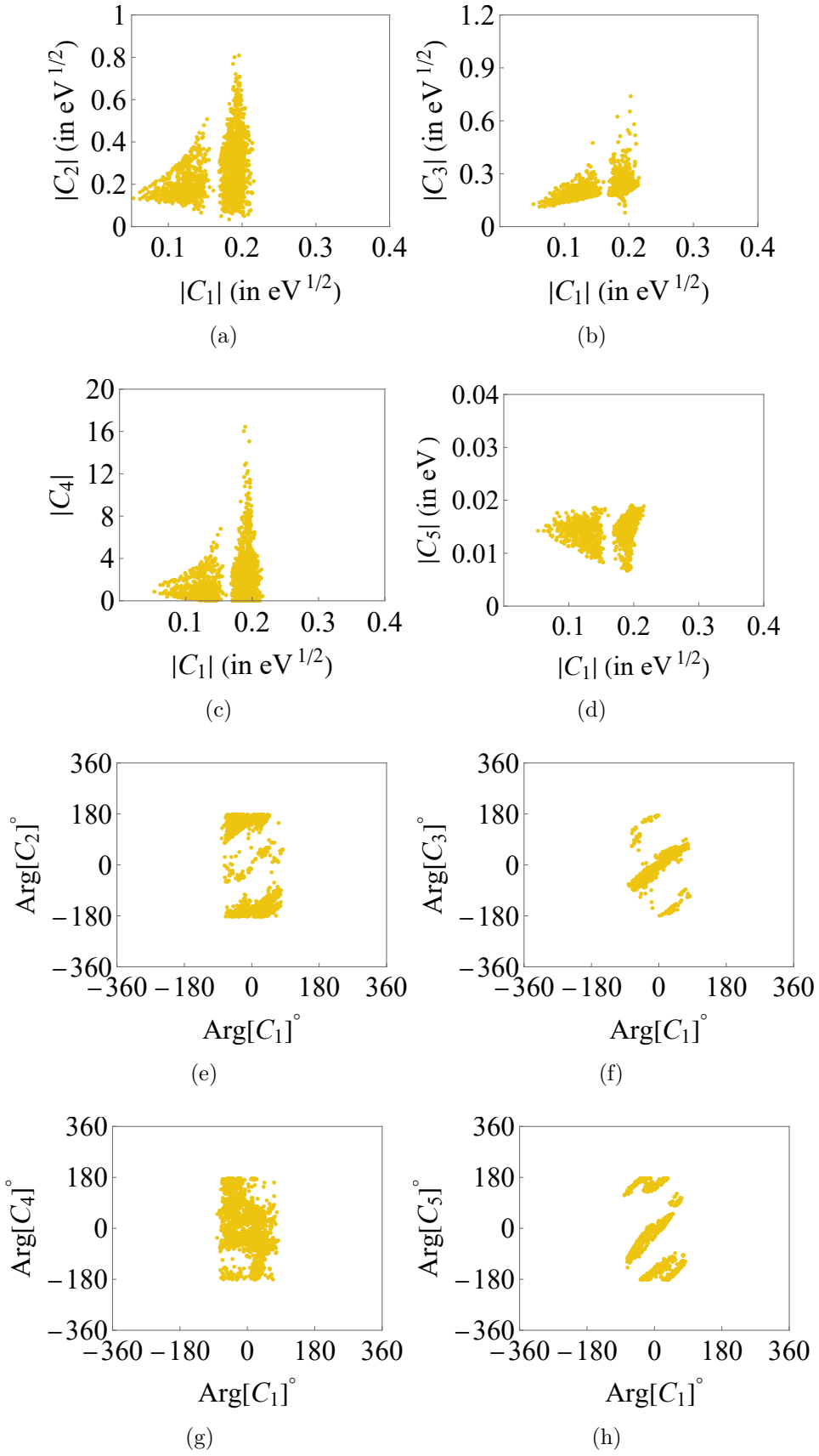


Figure 4. The correlation plots for the model parameter combinations in case of normal hierarchy of neutrino masses.

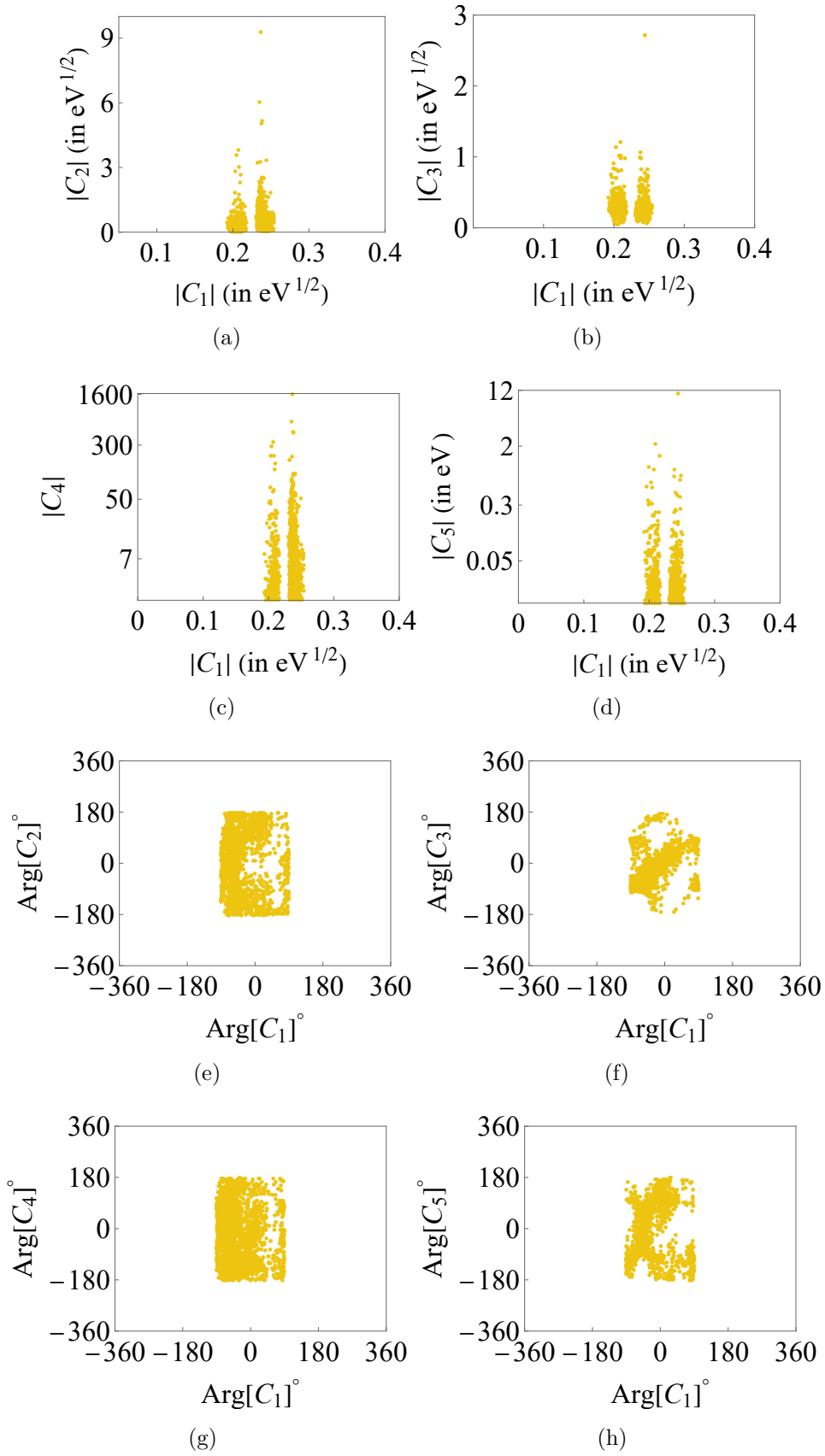


Figure 5. The correlation plots for the model parameter combinations in case of inverted hierarchy of neutrino masses.

Parameter	Minimum	Maximum
$ C_1 /\text{eV}^{\frac{1}{2}}$	0.192	0.254
$ C_2 /\text{eV}^{\frac{1}{2}}$	0.042	9.303
$ C_3 /\text{eV}^{\frac{1}{2}}$	0.064	2.720
$ C_4 $	0.0018	1.64×10^3
$ C_5 /\text{eV}$	0.0004	11.144
$\text{Arg}[C_1]/^\circ$	-89.996	89.699
$\text{Arg}[C_2]/^\circ$	-179.849	179.814
$\text{Arg}[C_3]/^\circ$	-168.629	176.350
$\text{Arg}[C_4]/^\circ$	-179.593	179.793
$\text{Arg}[C_5]/^\circ$	-178.116	179.754

Table 7. Represents the maximum and minimum values of the model parameters for inverted hierarchy of neutrino masses.

As mentioned earlier, $Re[d]$, $Im[d]$ and $Re[t]$ span M_ν and all the predictions associated with it. Hence, $m_{\beta\beta}$ is no exception. We calculate the numerical values of $m_{\beta\beta}$ for both normal and inverted hierarchy of neutrino masses. So far, we are aware of the upper bounds concerning this parameter from various experiments (see Table 8). The model predicts $m_{\beta\beta}$ values that lie within the limits established by combined analysis of GERDA [67] and KamLAND-Zen [68, 69] experiments. For normal hierarchy, our model predicts $m_{\beta\beta}$ values in the range of 0.0165 eV to 0.0311 eV, which is within the future sensitivity region of the LEGEND-1000 experiment [70]. In case of inverted hierarchy, the predicted range is 0.0482 eV to 0.0520 eV.

In Figs. 6(a) and 6(b), we show the values of $m_{\beta\beta}$ versus the lightest neutrino mass eigenvalues.

Isotope	$T_{1/2}$ (years)	$m_{\beta\beta}$ (eV)	Collaboration
^{82}Se	$> 3.5 \times 10^{24}$	$< 0.311 - 0.638$	CUPID-0 [71]
^{130}Te	$> 2.2 \times 10^{25}$	$< 0.09 - 0.305$	CUORE [72]
^{136}Xe	$> 3.5 \times 10^{25}$	$< 0.093 - 0.286$	EXO [73]
^{76}Ge	$> 1.8 \times 10^{26}$	$< 0.08 - 0.18$	GERDA [67]
^{136}Xe	$> 1.07 \times 10^{26}$	$< 0.061 - 0.165$	KamLAND-Zen [69]
	$> 2.3 \times 10^{26}$	$< 0.036 - 0.156$	[68]
^{76}Ge	$> 1.3 \times 10^{28}$	$< 0.09 - 0.21$	LEGEND-1000 [70]

Table 8. The present lower limits on the half life ($T_{1/2}$) and upper limits on the $m_{\beta\beta}$ of $0\nu\beta\beta$ decay for different isotopes.

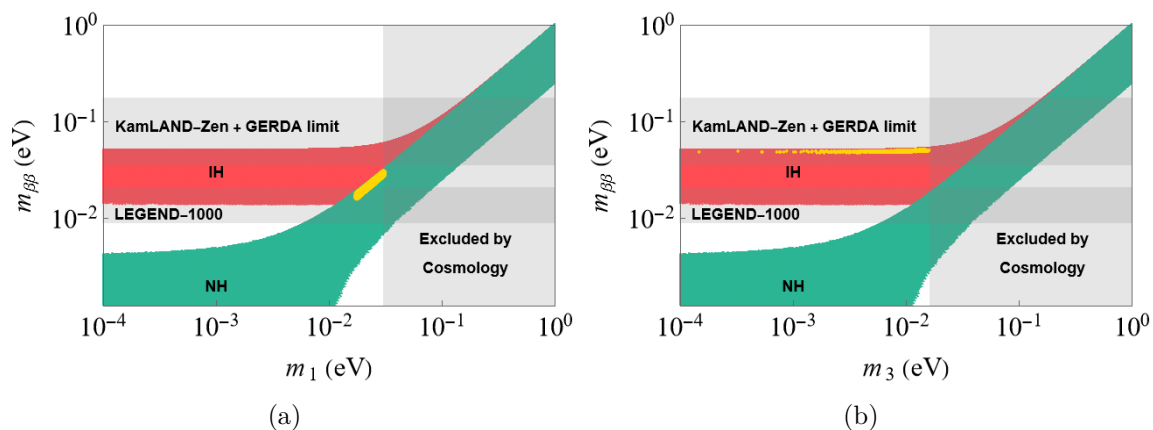


Figure 6. The plots for $m_{\beta\beta}$ versus the lightest neutrino mass eigenvalue: (a) for normal hierarchy (b) for inverted hierarchy. In the plots, the red and green bands show the regions allowed by current oscillation data, the gray bands indicate the bounds on $m_{\beta\beta}$ and the lowest neutrino mass eigenvalues, and the ‘bright yellow’ plot represent the model’s prediction.

5 Charged Lepton Flavour Violation

In the SM of Particle Physics, cLFV processes [74–76] are incredibly rare, with predicted branching ratios around 10^{-50} . Thus, cLFV is one of the most interesting probes of physics beyond the SM. Among the various decay channels, transitions involving muons, are the promising ones because muons are abundantly produced in cosmic radiation and accelerators, and they have a longer lifetime than other leptons, making them ideal for study. In the present work, we study the dominant decay, $\mu \rightarrow e\gamma$. The current best limit on the branching ratio of this decay is set by MEG experiment [77]: $BR(\mu \rightarrow e\gamma) < 4.2 \times 10^{-13}$ (90% CL). The MEG II [78–80] collaboration is searching for this decay at the Paul Scherrer Institut (PSI) muon beam facility. Their goal is to improve the sensitivity of their measurements to achieve a branching ratio : $BR(\mu \rightarrow e\gamma) < 6 \times 10^{-14}$ (90% CL) by the end of 2026. To complement these experimental efforts, it’s worthwhile to explore theoretical beyond standard models that could explain or predict these rare decays.

Having said that, as we consider the Type-I and Type-II seesaw mechanisms in our model, we may therefore analyze how each mechanism contributes to the $\mu \rightarrow e\gamma$ decay. We then try to see which contribution is the dominant one.

In the case of Type-I seesaw, the possibility of $\mu \rightarrow e\gamma$ decay arises due to the existence of light-heavy neutrino mixing. The expression for branching ratio for the Type-I seesaw is written as [81–85],

$$BR(\mu \rightarrow e\gamma) = \frac{3\alpha_f}{8\pi} \left| \sum_i K_{ei} K_{i\mu}^\dagger F \left(\frac{M_i^2}{M_W^2} \right) \right|^2, \quad (5.1)$$

where, α_f is the fine structure constant, K represents the light-heavy mixing matrix, M_i is the mass of the right handed neutrinos and M_W is the mass of W^\pm . The form factor $F(x)$ is expressed as,

$$F(x) = \frac{x(1 - 6x + 3x^2 + 2x^3 - 6x^2 \ln x)}{2(1 - x)^4}, \quad (5.2)$$

where, $x = \frac{M_i^2}{M_W^2}$. It is important to mention that the branching ratio is dependent on $K = M_D^\dagger (M_R^\dagger)^{-1} U_R$, where U_R is the matrix which diagonalises M_R . Therefore, the contribution to this decay is dependent on the flavour structure of the neutrino mass matrices, M_D and M_R . In our model, M_D is a diagonal matrix. For there to be a significant and non vanishing contribution to the branching ratio, M_R should have non-zero entries in the (1, 1), (1, 2), (1, 3), (2, 2) and (2, 3) positions. However, the structure of M_R in our model is such that (1, 2) and (1, 3) are vanishing entries, which forces the matrix element $K_{ei} K_{i\mu}^\dagger$ to be zero. So, we conclude that the Type-I contribution to the $\mu \rightarrow e\gamma$ decay is zero in our model.

With this inference in mind, let's now shift our focus to the Type-II seesaw contribution to the branching ratio of $\mu \rightarrow e\gamma$ decay. In the Type-II case, this process occurs at the one loop level, involving the doubly and singly charged components of the triplet Higgs, Δ . The branching ratio for this process is given by [86–88],

$$BR(\mu \rightarrow e\gamma) = \frac{\alpha_f |(Y^* Y)_{e\mu}^2|}{192\pi G_F^2} \left(\frac{1}{m_{\Delta^+}^2} + \frac{8}{m_{\Delta^{++}}^2} \right)^2. \quad (5.3)$$

In the above equation, Y is the Type-II Yukawa matrix, G_F is the Fermi constant, m_{Δ^+} is the mass of the singly charged component of the triplet field and $m_{\Delta^{++}}$ stands for the mass of the doubly charged component of the triplet field. In our analysis we assume small differences between the components of Δ , which means, $m_{\Delta^+} \simeq m_{\Delta^{++}} = m_\Delta$. With this assumption and using the value of $(Y^* Y)_{e\mu}$ from the model, the branching ratio takes the following form,

$$BR(\mu \rightarrow e\gamma) \simeq 0.659 \frac{\alpha_f}{\pi G_F^2} \left(\frac{|C_5|}{m_\Delta v_\Delta} \right)^4. \quad (5.4)$$

From Eq.,(5.4), we understand that the branching ratio depends on the Type-II parameter, C_5 . Given the experimental sensitivities of $BR(\mu \rightarrow e\gamma)$ and the values of C_5 predicted by this model, we determine the possible numerical ranges of m_Δ and v_Δ . These values are summarized in Table 9.

Based on the values in Table 9, we understand that the $BR(\mu \rightarrow e\gamma)$ predicted by our model is consistent with the upper bounds set by the MEG and MEG-II experiments, suggesting that m_Δ lies approximately between 123 GeV and 10^4 GeV (1 TeV). This implies that detecting the decay in the ongoing searches at MEG-II [78–80] experiment could set limits on the masses of doubly or singly charged scalars, likely between 123 GeV and 10^4 GeV (1 TeV). To better understand these findings, we highlight the Figs. 7(a) and 7(b).

Parameter	Normal hierarchy		Inverted hierarchy	
	Minimum	Maximum	Minimum	Maximum
$BR(\mu \rightarrow e\gamma)$	10^{-16}	7.70×10^{-13}	10^{-16}	6.94×10^{-13}
m_Δ	140 GeV	10^4 GeV	123 GeV	10^4 GeV
v_Δ	1 eV	6.97 eV	1 eV	6.98 eV
$ C_5 $	0.0078 eV	0.0191 eV	0.0026 eV	0.7770 eV

Table 9. Table with the model predictions for the $\mu \rightarrow e\gamma$ decay in case of normal and inverted hierarchies.

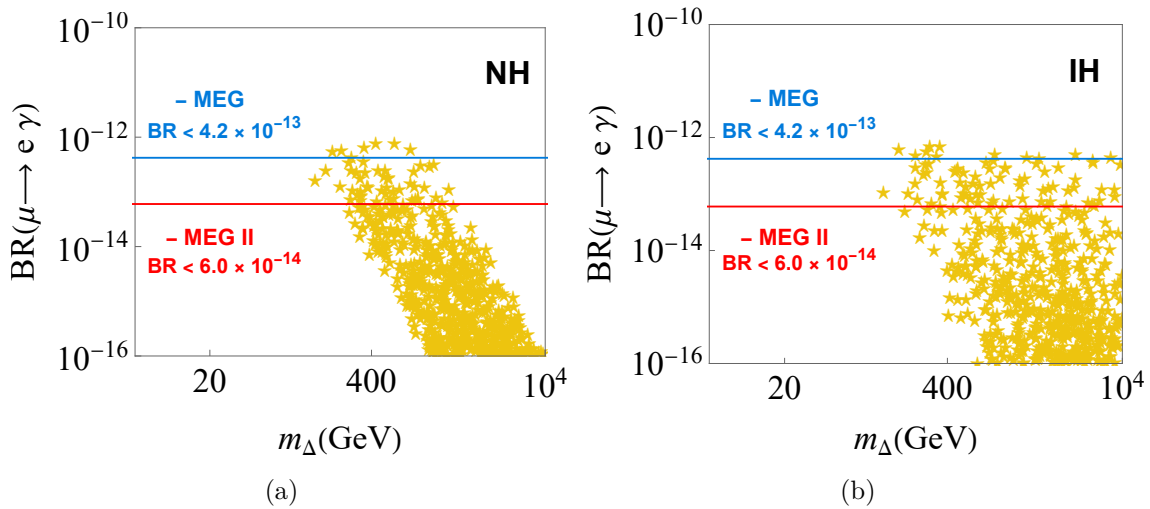


Figure 7. $BR(\mu \rightarrow e\gamma)$ versus m_Δ , where $m_\Delta = m_{\Delta^{++}} \simeq m_{\Delta^+}$ in this model: (a) for normal hierarchy (b) for inverted hierarchy. In the plots, blue and red lines represent the sensitivities of MEG and MEG-II respectively. The ‘dark yellow’ stars (\star) are the predictions of our model.

6 Summary and Discussions

In this paper, we have constructed a neutrino mass matrix model based on the extension of the Standard Model with $\Delta(27)$ symmetry in a Type-I + Type-II framework. An additional Z_{10} symmetry has been introduced to prevent certain unfavourable terms from appearing in the Yukawa lagrangian. The mass matrix in our model exhibits a broken μ - τ symmetry and contains only *three real and independent texture parameters* that collectively describe the entire mass matrix and its associated predictions.

To derive the phenomenology associated with the texture, we have conducted our analysis for both normal and inverted hierarchies of neutrino masses. In this regard, we have used the 3σ values for the mixing angles and the Dirac CP phase as inputs. However, we have observed that the model naturally restricts θ_{23} to specific ranges of values in the case of normal hierarchy. This is one of the highlighting features of

our model.

Furthermore, our model predicts the three neutrino mass eigenvalues and allows the two Majorana phases to vary approximately between -90° and 90° . To test our model on experimental grounds, we have extended our discussion in the light of neutrino-less double beta ($0\nu\beta\beta$) decay and charged lepton flavour violation (cLFV). Our model predicts the highest possible values for $m_{\beta\beta}$ to be 0.0311 eV and 0.0520 eV for normal and inverted hierarchies, respectively, which are consistent with the experimental upper bounds.

In the context of cLFV, we explore our model's contribution to the $\mu \rightarrow e\gamma$ decay. In this study, we observe an interesting result: due to the presence of texture zeros in the structure of M_R , the Type-I seesaw mechanism provides no contribution to this decay. Only the Type-II seesaw mechanism offers a non-zero contribution to the branching ratio, and we have explored the values of m_Δ for which the branching ratio is consistent with current and future experimental sensitivities. From the study we have found that m_Δ lies approximately between 123 GeV and 10^4 GeV (1 TeV).

Acknowledgements

MD would like to thank R. Srivastava, Department of Physics, IISER-Bhopal, for an important discussion related to the $\Delta(27)$ symmetry group, and B. Karmakar, University of Silesia, Katowice, for a few discussions related to cLFV. The research work of MD is financially supported by Council of Scientific and Industrial Research (CSIR), Government of India through a NET Junior Research Fellowship vide grant No. 09/0059(15346)/2022-EMR-I.

References

- [1] C.L. Cowan, F. Reines, F.B. Harrison, H.W. Kruse and A.D. McGuire, *Detection of the free neutrino: A Confirmation*, *Science* **124** (1956) 103.
- [2] B. Pontecorvo, *Mesonium and anti-mesonium*, *Sov. Phys. JETP* **6** (1957) 429.
- [3] SNO collaboration, *Direct evidence for neutrino flavor transformation from neutral current interactions in the Sudbury Neutrino Observatory*, *Phys. Rev. Lett.* **89** (2002) 011301 [[nucl-ex/0204008](#)].
- [4] KAMLAND collaboration, *First results from KamLAND: Evidence for reactor anti-neutrino disappearance*, *Phys. Rev. Lett.* **90** (2003) 021802 [[hep-ex/0212021](#)].
- [5] SUPER-KAMIOKANDE collaboration, *Measurement of the flux and zenith angle distribution of upward through going muons by Super-Kamiokande*, *Phys. Rev. Lett.* **82** (1999) 2644 [[hep-ex/9812014](#)].
- [6] M. Yoshimura, *Unified Gauge Theories and the Baryon Number of the Universe*, *Phys. Rev. Lett.* **41** (1978) 281.

- [7] E.K. Akhmedov, G.C. Branco and M.N. Rebelo, *Seesaw mechanism and structure of neutrino mass matrix*, *Phys. Lett. B* **478** (2000) 215 [[hep-ph/9911364](#)].
- [8] Y. Cai, T. Han, T. Li and R. Ruiz, *Lepton Number Violation: Seesaw Models and Their Collider Tests*, *Front. in Phys.* **6** (2018) 40 [[1711.02180](#)].
- [9] R.N. Mohapatra, *Seesaw mechanism and its implications*, in *SEESAW25: International Conference on the Seesaw Mechanism and the Neutrino Mass*, pp. 29–44, 12, 2004, DOI [[hep-ph/0412379](#)].
- [10] S.F. King and C. Luhn, *Neutrino Mass and Mixing with Discrete Symmetry*, *Rept. Prog. Phys.* **76** (2013) 056201 [[1301.1340](#)].
- [11] R.N. Mohapatra and A.Y. Smirnov, *Neutrino Mass and New Physics*, *Ann. Rev. Nucl. Part. Sci.* **56** (2006) 569 [[hep-ph/0603118](#)].
- [12] S.F. King, *Neutrino mass models*, *Rept. Prog. Phys.* **67** (2004) 107 [[hep-ph/0310204](#)].
- [13] A. Melfo, M. Nemevsek, F. Nesti, G. Senjanovic and Y. Zhang, *Type II Seesaw at LHC: The Roadmap*, *Phys. Rev. D* **85** (2012) 055018 [[1108.4416](#)].
- [14] P. Fileviez Perez, T. Han, G.-y. Huang, T. Li and K. Wang, *Neutrino Masses and the CERN LHC: Testing Type II Seesaw*, *Phys. Rev. D* **78** (2008) 015018 [[0805.3536](#)].
- [15] T.P. Cheng and L.-F. Li, *Neutrino Masses, Mixings and Oscillations in $SU(2) \times U(1)$ Models of Electroweak Interactions*, *Phys. Rev. D* **22** (1980) 2860.
- [16] E.K. Akhmedov and M. Frigerio, *Interplay of type I and type II seesaw contributions to neutrino mass*, *JHEP* **01** (2007) 043 [[hep-ph/0609046](#)].
- [17] C.-F. Wong and Y. Chen, *Tree level Majorana neutrino mass from Type-1 \times Type-2 Seesaw mechanism with Dark Matter*, *Phys. Lett. B* **833** (2022) 137354 [[2205.08531](#)].
- [18] M. Kashav and S. Verma, *A_4 Flavor Model for Deviation in $\mu - \tau$ Reflection Symmetry with Type-I+II Seesaw Extensions*, *Int. J. Theor. Phys.* **62** (2023) 267.
- [19] V. Banerjee and S. Mishra, *Interplay of type-I and type-II seesaw in neutrinoless double beta decay in left-right symmetric model*, [2309.11105](#).
- [20] P. Ramond, R.G. Roberts and G.G. Ross, *Stitching the Yukawa quilt*, *Nucl. Phys. B* **406** (1993) 19 [[hep-ph/9303320](#)].
- [21] A. Ibarra and G. Ross, *Predicting neutrino parameters from texture zeros*, *PoS AHEP2003* (2003) 030.
- [22] P.O. Ludl and W. Grimus, *A complete survey of texture zeros in the lepton mass matrices*, *JHEP* **07** (2014) 090 [[1406.3546](#)].
- [23] P.F. Harrison, D.H. Perkins and W.G. Scott, *Tri-bimaximal mixing and the neutrino oscillation data*, *Phys. Lett. B* **530** (2002) 167 [[hep-ph/0202074](#)].
- [24] E. Ma, *Tribimaximal neutrino mixing from a supersymmetric model with A_4 family symmetry*, *Phys. Rev. D* **73** (2006) 057304 [[hep-ph/0511133](#)].

- [25] Y. Lin, *Tri-bimaximal Neutrino Mixing from $A(4)$ and $\theta_{13} \sim \theta(C)$* , *Nucl. Phys. B* **824** (2010) 95 [0905.3534].
- [26] Z.-z. Xing, *Flavor structures of charged fermions and massive neutrinos*, *Phys. Rept.* **854** (2020) 1 [1909.09610].
- [27] M. Dey, P. Chakraborty and S. Roy, *The μ - τ mixed symmetry and neutrino mass matrix*, *Phys. Lett. B* **839** (2023) 137767 [2211.01314].
- [28] Z.-z. Xing, *The μ - τ reflection symmetry of Majorana neutrinos **, *Rept. Prog. Phys.* **86** (2023) 076201 [2210.11922].
- [29] Z.-C. Liu, C.-X. Yue and Z.-h. Zhao, *Neutrino $\mu - \tau$ reflection symmetry and its breaking in the minimal seesaw*, *JHEP* **10** (2017) 102 [1707.05535].
- [30] Z.-z. Xing and Z.-h. Zhao, *A review of μ - τ flavor symmetry in neutrino physics*, *Rept. Prog. Phys.* **79** (2016) 076201 [1512.04207].
- [31] G.C. Branco, J.M. Gerard and W. Grimus, *GEOMETRICAL T VIOLATION*, *Phys. Lett. B* **136** (1984) 383.
- [32] E. Ma, *Near tribimaximal neutrino mixing with $\Delta(27)$ symmetry*, *Phys. Lett. B* **660** (2008) 505 [0709.0507].
- [33] M. Abbas and S. Khalil, *Fermion masses and mixing in $\Delta(27)$ flavour model*, *Phys. Rev. D* **91** (2015) 053003 [1406.6716].
- [34] P. Chen, G.-J. Ding, A.D. Rojas, C.A. Vaquera-Araujo and J.W.F. Valle, *Warped flavor symmetry predictions for neutrino physics*, *JHEP* **01** (2016) 007 [1509.06683].
- [35] S. Centelles Chuliá, R. Srivastava and J.W.F. Valle, *CP violation from flavor symmetry in a lepton quarticity dark matter model*, *Phys. Lett. B* **761** (2016) 431 [1606.06904].
- [36] V.V. Vien and D.P. Khoi, *$U(1)_{B-L}$ extension based on $\Delta(27)$ symmetry for lepton masses and mixings*, *Mod. Phys. Lett. A* **35** (2020) 2050181.
- [37] E. Ma and G. Rajasekaran, *Softly broken $A(4)$ symmetry for nearly degenerate neutrino masses*, *Phys. Rev. D* **64** (2001) 113012 [hep-ph/0106291].
- [38] S.F. King and M. Malinsky, *$A(4)$ family symmetry and quark-lepton unification*, *Phys. Lett. B* **645** (2007) 351 [hep-ph/0610250].
- [39] G. Altarelli and F. Feruglio, *Discrete Flavor Symmetries and Models of Neutrino Mixing*, *Rev. Mod. Phys.* **82** (2010) 2701 [1002.0211].
- [40] E. Ma, *Lepton family symmetry and neutrino mass matrix*, *Mod. Phys. Lett. A* **19** (2004) 577 [hep-ph/0401025].
- [41] B. Hu, F. Wu and Y.-L. Wu, *$Z(3)$ Symmetry and Neutrino Mixing in Type II Seesaw*, *Phys. Rev. D* **75** (2007) 113003 [hep-ph/0612344].
- [42] A.E. Cárcamo Hernández and I. de Medeiros Varzielas, *$\Delta(27)$ framework for cobimaximal neutrino mixing models*, *Phys. Lett. B* **806** (2020) 135491 [2003.01134].

- [43] M. Dey and S. Roy, *A Realistic Neutrino mixing scheme arising from A_4 symmetry*, [2304.07259](#).
- [44] M. Dey and S. Roy, *Revisiting the Dirac Nature of Neutrinos*, [2403.12461](#).
- [45] C.D. Froggatt and H.B. Nielsen, *Hierarchy of Quark Masses, Cabibbo Angles and CP Violation*, *Nucl. Phys. B* **147** (1979) 277.
- [46] K.S. Babu and S. Nandi, *Natural fermion mass hierarchy and new signals for the Higgs boson*, *Phys. Rev. D* **62** (2000) 033002 [[hep-ph/9907213](#)].
- [47] J.D. Lykken, Z. Murdock and S. Nandi, *A light scalar as the messenger of electroweak and flavor symmetry breaking*, *Phys. Rev. D* **79** (2009) 075014 [[0812.1826](#)].
- [48] C. Hagedorn and R. Ziegler, *$\mu - \tau$ Symmetry and Charged Lepton Mass Hierarchy in a Supersymmetric D_4 Model*, *Phys. Rev. D* **82** (2010) 053011 [[1007.1888](#)].
- [49] J. Ganguly, *Fermion mass hierarchy and lepton flavor violation using CP symmetry*, *Int. J. Mod. Phys. A* **37** (2022) 2250095 [[2205.03084](#)].
- [50] C. Bonilla, A.E. Carcamo Hernandez, S. Kovalenko, H. Lee, R. Pasechnik and I. Schmidt, *Fermion mass hierarchy in an extended left-right symmetric model*, *JHEP* **12** (2023) 075 [[2305.11967](#)].
- [51] A.E. Cárcamo Hernández, I. de Medeiros Varzielas and J.M. González, *Predictive linear seesaw model with $\Delta(27)$ family symmetry*, [2401.15147](#).
- [52] PARTICLE DATA GROUP collaboration, *Review of Particle Physics*, *Phys. Rev. D* **98** (2018) 030001.
- [53] PARTICLE DATA GROUP collaboration, *Review of Particle Physics*, *PTEP* **2022** (2022) 083C01.
- [54] Z. Maki, M. Nakagawa and S. Sakata, *Remarks on the unified model of elementary particles*, *Prog. Theor. Phys.* **28** (1962) 870.
- [55] I. Esteban, M.C. Gonzalez-Garcia, M. Maltoni, T. Schwetz and A. Zhou, *The fate of hints: updated global analysis of three-flavor neutrino oscillations*, *JHEP* **09** (2020) 178 [[2007.14792](#)].
- [56] M.C. Gonzalez-Garcia, M. Maltoni and T. Schwetz, *NuFIT: Three-Flavour Global Analyses of Neutrino Oscillation Experiments*, *Universe* **7** (2021) 459 [[2111.03086](#)].
- [57] PLANCK collaboration, *Planck 2018 results. VI. Cosmological parameters*, *Astron. Astrophys.* **641** (2020) A6 [[1807.06209](#)].
- [58] J. Schechter and J.W.F. Valle, *Neutrinoless Double beta Decay in $SU(2) \times U(1)$ Theories*, *Phys. Rev. D* **25** (1982) 2951.
- [59] M. Blennow, E. Fernandez-Martinez, J. Lopez-Pavon and J. Menendez, *Neutrinoless double beta decay in seesaw models*, *JHEP* **07** (2010) 096 [[1005.3240](#)].
- [60] J.D. Vergados, H. Ejiri and F. Simkovic, *Theory of Neutrinoless Double Beta Decay*, *Rept. Prog. Phys.* **75** (2012) 106301 [[1205.0649](#)].

- [61] S.M. Bilenky and C. Giunti, *Neutrinoless double-beta decay: A brief review*, *Mod. Phys. Lett. A* **27** (2012) 1230015 [[1203.5250](#)].
- [62] F.F. Deppisch, M. Hirsch and H. Pas, *Neutrinoless Double Beta Decay and Physics Beyond the Standard Model*, *J. Phys. G* **39** (2012) 124007 [[1208.0727](#)].
- [63] S.M. Bilenky and C. Giunti, *Neutrinoless Double-Beta Decay: a Probe of Physics Beyond the Standard Model*, *Int. J. Mod. Phys. A* **30** (2015) 1530001 [[1411.4791](#)].
- [64] M.J. Dolinski, A.W.P. Poon and W. Rodejohann, *Neutrinoless Double-Beta Decay: Status and Prospects*, *Ann. Rev. Nucl. Part. Sci.* **69** (2019) 219 [[1902.04097](#)].
- [65] M. Agostini, G. Benato, J.A. Detwiler, J. Menéndez and F. Vissani, *Toward the discovery of matter creation with neutrinoless $\beta\beta$ decay*, *Rev. Mod. Phys.* **95** (2023) 025002 [[2202.01787](#)].
- [66] A. Barabash, *Double Beta Decay Experiments: Recent Achievements and Future Prospects*, *Universe* **9** (2023) 290.
- [67] GERDA collaboration, *Final Results of GERDA on the Search for Neutrinoless Double- β Decay*, *Phys. Rev. Lett.* **125** (2020) 252502 [[2009.06079](#)].
- [68] KAMLAND-ZEN collaboration, *Search for the Majorana Nature of Neutrinos in the Inverted Mass Ordering Region with KamLAND-Zen*, *Phys. Rev. Lett.* **130** (2023) 051801 [[2203.02139](#)].
- [69] KAMLAND-ZEN collaboration, *Search for Majorana Neutrinos near the Inverted Mass Hierarchy Region with KamLAND-Zen*, *Phys. Rev. Lett.* **117** (2016) 082503 [[1605.02889](#)].
- [70] LEGEND collaboration, *The Large Enriched Germanium Experiment for Neutrinoless $\beta\beta$ Decay: LEGEND-1000 Preconceptual Design Report*, [2107.11462](#).
- [71] CUPID collaboration, *Final result of CUPID-0 phase-I in the search for the ^{82}Se Neutrinoless Double- β Decay*, *Phys. Rev. Lett.* **123** (2019) 032501 [[1906.05001](#)].
- [72] CUORE collaboration, *Search for Majorana neutrinos exploiting millikelvin cryogenics with CUORE*, *Nature* **604** (2022) 53 [[2104.06906](#)].
- [73] EXO-200 collaboration, *Search for Neutrinoless Double- β Decay with the Complete EXO-200 Dataset*, *Phys. Rev. Lett.* **123** (2019) 161802 [[1906.02723](#)].
- [74] L. Calibbi and G. Signorelli, *Charged Lepton Flavour Violation: An Experimental and Theoretical Introduction*, *Riv. Nuovo Cim.* **41** (2018) 71 [[1709.00294](#)].
- [75] M. Ardu and G. Pezzullo, *Introduction to Charged Lepton Flavor Violation*, *Universe* **8** (2022) 299 [[2204.08220](#)].
- [76] F. Cei and D. Nicolo, *Lepton Flavour Violation Experiments*, *Adv. High Energy Phys.* **2014** (2014) 282915.
- [77] MEG collaboration, *Search for the lepton flavour violating decay $\mu^+ \rightarrow e + \gamma$ with the full dataset of the MEG experiment*, *Eur. Phys. J. C* **76** (2016) 434 [[1605.05081](#)].

- [78] MEG II collaboration, *MEG II experiment status and prospect*, *PoS NuFact2021* (2022) 120 [2201.08200].
- [79] MEG II collaboration, *A search for $\mu^+ \rightarrow e + \gamma$ with the first dataset of the MEG II experiment*, *Eur. Phys. J. C* **84** (2024) 216 [2310.12614].
- [80] MEG II collaboration, *Status of the MEG II experiment*, *PoS EPS-HEP2023* (2024) 355.
- [81] S.M. Bilenky, S.T. Petcov and B. Pontecorvo, *Lepton Mixing, $\mu \rightarrow e + \gamma$ Decay and Neutrino Oscillations*, *Phys. Lett. B* **67** (1977) 309.
- [82] A. Ilakovac and A. Pilaftsis, *Flavor violating charged lepton decays in seesaw-type models*, *Nucl. Phys. B* **437** (1995) 491 [hep-ph/9403398].
- [83] D. Tommasini, G. Barenboim, J. Bernabeu and C. Jarlskog, *Nondecoupling of heavy neutrinos and lepton flavor violation*, *Nucl. Phys. B* **444** (1995) 451 [hep-ph/9503228].
- [84] D.V. Forero, S. Morisi, M. Tortola and J.W.F. Valle, *Lepton flavor violation and non-unitary lepton mixing in low-scale type-I seesaw*, *JHEP* **09** (2011) 142 [1107.6009].
- [85] A. Datta, B. Karmakar and A. Sil, *Flavored leptogenesis and neutrino mass with A_4 symmetry*, *JHEP* **12** (2021) 051 [2106.06773].
- [86] D.N. Dinh, A. Ibarra, E. Molinaro and S.T. Petcov, *The $\mu - e$ Conversion in Nuclei, $\mu \rightarrow e\gamma$, $\mu \rightarrow 3e$ Decays and TeV Scale See-Saw Scenarios of Neutrino Mass Generation*, *JHEP* **08** (2012) 125 [1205.4671].
- [87] M.M. Ferreira, T.B. de Melo, S. Kovalenko, P.R.D. Pinheiro and F.S. Queiroz, *Lepton Flavor Violation and Collider Searches in a Type I + II Seesaw Model*, *Eur. Phys. J. C* **79** (2019) 955 [1903.07634].
- [88] N.D. Barrie and S.T. Petcov, *Lepton Flavour Violation tests of Type II Seesaw Leptogenesis*, *JHEP* **01** (2023) 001 [2210.02110].

A Appendix

A.1 The Pontecorvo-Maki-Nakagawa-Sakata matrix

The Pontecorvo-Maki-Nakagawa-Sakata (PMNS) matrix is a 3×3 unitary matrix which is parametrised in terms of mixing angles and phases. The parametrisation of the PMNS matrix (U) adopted by the Particle Data Group [52] is shown below,

$$U = P_\phi \cdot \tilde{U} \cdot P_M, \quad (\text{A.1})$$

we demarcate U which is the general one, from the \tilde{U} that excludes the phases, where, $P_M = \text{diag}(e^{i\alpha}, e^{i\beta}, 1)$ contains the two Majorana phases, α and β . The arbitrary phase matrix $P_\phi = \text{diag}(e^{i\phi_1}, e^{i\phi_2}, e^{i\phi_3})$, contains three arbitrary phases ($\phi_{i=1,2,3}$), and

the latter can be eliminated from U by redefining the charged lepton fields in terms of these phases. Hence, the PMNS matrix after redefinition of the said phases, attains the following form,

$$U = \tilde{U}.P_M. \quad (\text{A.2})$$

The matrix \tilde{U} is written in its standard form, in the following manner,

$$\tilde{U} = \begin{bmatrix} 1 & 0 & 0 \\ 0 & c_{23} & s_{23} \\ 0 & -s_{23} & c_{23} \end{bmatrix} \times \begin{bmatrix} c_{13} & 0 & s_{13} e^{-i\delta} \\ 0 & 1 & 0 \\ -s_{13} e^{i\delta} & 0 & c_{13} \end{bmatrix} \times \begin{bmatrix} c_{12} & s_{12} & 0 \\ -s_{12} & c_{12} & 0 \\ 0 & 0 & 1 \end{bmatrix}, \quad (\text{A.3})$$

where, s_{ij} and c_{ij} represents $\sin \theta_{ij}$ and $\cos \theta_{ij}$ respectively. If the charged lepton mass matrix is already diagonal, then usually, the matrix U is the diagonalising matrix for M_ν , i.e,

$$U^T.M_\nu.U = \text{diag}(m_1, m_2, m_3), \quad (\text{A.4})$$

However, we rearrange the above equation in the following way,

$$\tilde{U}^T.M_\nu.\tilde{U} = \text{diag}(\tilde{m}_1, \tilde{m}_2, m_3), \quad (\text{A.5})$$

such that, $\tilde{m}_1 = m_1 e^{-2i\alpha}$ and $\tilde{m}_2 = m_2 e^{-2i\beta}$. In the present model, \tilde{U} is the PMNS matrix which diagonalises the neutrino mass matrix M_ν .

A.2 $\Delta(27)$ group

We briefly explore the product rules associated with $\Delta(27)$ symmetry,

$$\begin{aligned} 3 \otimes 3 &= \bar{3}_{s_1} \oplus \bar{3}_{s_2} \oplus \bar{3}_a, \\ \bar{3} \otimes \bar{3} &= 3_{s_1} \oplus 3_{s_2} \oplus 3_a, \\ 3 \otimes \bar{3} &= \sum_{r=0}^2 1_{r,0} \oplus \sum_{r=0}^2 1_{r,1} \oplus \sum_{r=0}^2 1_{r,2}, \\ 1_{p,q} \otimes 1_{p',q'} &= 1_{(p+p') \bmod 3, (q+q') \bmod 3}. \end{aligned} \quad (\text{A.6})$$

If (a_1, a_2, a_3) and (b_1, b_2, b_3) are two triplets under $\Delta(27)$ then,

$$\begin{aligned} (3 \otimes 3)_{\bar{3}_{s_1}} &= (a_1 b_1, a_2 b_2, a_3 b_3), \\ (3 \otimes 3)_{\bar{3}_{s_2}} &= \frac{1}{2}(a_2 b_3 + a_3 b_2, a_3 b_1 + a_1 b_3, a_1 b_2 + a_2 b_1), \\ (3 \otimes 3)_{\bar{3}_a} &= \frac{1}{2}(a_2 b_3 - a_3 b_2, a_3 b_1 - a_1 b_3, a_1 b_2 - a_2 b_1), \\ (3 \otimes \bar{3})_{1_{r,0}} &= a_1 b_1 + \omega^{2r} a_2 b_2 + \omega^r a_3 b_3, \\ (3 \otimes \bar{3})_{1_{r,1}} &= a_1 b_2 + \omega^{2r} a_2 b_3 + \omega^r a_3 b_1, \\ (3 \otimes \bar{3})_{1_{r,2}} &= a_1 b_3 + \omega^{2r} a_2 b_1 + \omega^r a_3 b_2, \end{aligned} \quad (\text{A.7})$$

where, $r = 0, 1, 2$ and $\omega = e^{\frac{2\pi i}{3}}$.

A.3 Z_{10} group

Z_{10} group, represents a modulus symmetry and it involves the elements 0 to 9. If, x_1 and x_2 are two group elements of Z_{10} , then under group operation:

$$x_1 \times x_2 = (x_1 + x_2) \text{ mod } 10. \quad (\text{A.8})$$

The irreducible representation of a general group element (x), is given by: $e^{2x\pi i/10}$. In Table 10, we show the multiplication table of the Z_{10} group,

Z_{10}	0	1	2	3	4	5	6	7	8	9
0	0	1	2	3	4	5	6	7	8	9
1	1	2	3	4	5	6	7	8	9	0
2	2	3	4	5	6	7	8	9	0	1
3	3	4	5	6	7	8	9	0	1	2
4	4	5	6	7	8	9	0	1	2	3
5	5	6	7	8	9	0	1	2	3	4
6	6	7	8	9	0	1	2	3	4	5
7	7	8	9	0	1	2	3	4	5	6
8	8	9	0	1	2	3	4	5	6	7
9	9	0	1	2	3	4	5	6	7	8

Table 10. Represents the multiplication table of the Z_{10} group.

A.4 Scalar Potential

The scalar potential of our model which is invariant under $SU(2)_L \times \Delta(27) \times Z_{10}$ is presented as shown:

$$V = V(H) + V(\chi) + V(\Delta) + V(\eta) + V(\kappa) + V(\xi) + V(\zeta) + V(\varrho) + V(\text{interaction}).$$

Writing the terms explicitly, we have,

$$V(H) = -\mu_H^2(H^\dagger H) + \lambda^H(H^\dagger H)(H^\dagger H),$$

$$V(\chi) = \mu_\chi^2(\chi^\dagger \chi) + \lambda_1^\chi(\chi^\dagger \chi)(\chi^\dagger \chi) + \lambda_2^\chi(\chi^\dagger \chi)_{110}(\chi^\dagger \chi)_{120} + \lambda_3^\chi(\chi^\dagger \chi)_{101}(\chi^\dagger \chi)_{102} + \lambda_4^\chi(\chi^\dagger \chi)_{111}(\chi^\dagger \chi)_{122} + \lambda_5^\chi(\chi^\dagger \chi)_{121}(\chi^\dagger \chi)_{112},$$

$$V(\Delta) = \mu_\Delta^2 Tr(\Delta^\dagger \Delta) + \lambda_1^\Delta Tr(\Delta^\dagger \Delta)Tr(\Delta^\dagger \Delta) + \lambda_2^\Delta Tr(\Delta^\dagger \Delta)_{110}Tr(\Delta^\dagger \Delta)_{120} + \lambda_3^\Delta Tr(\Delta^\dagger \Delta)_{101}Tr(\Delta^\dagger \Delta)_{102} + \lambda_4^\Delta Tr(\Delta^\dagger \Delta)_{111}Tr(\Delta^\dagger \Delta)_{122} + \lambda_5^\Delta Tr(\Delta^\dagger \Delta)_{121}Tr(\Delta^\dagger \Delta)_{112},$$

$$V(\eta) = \mu_\eta^2(\eta^\dagger \eta) + \lambda^\eta(\eta^\dagger \eta)^2,$$

$$V(\kappa) = \mu_\kappa^2(\kappa^\dagger \kappa) + \lambda^\kappa(\kappa^\dagger \kappa)^2,$$

$$V(\xi) = \mu_\xi^2(\xi^\dagger \xi) + \lambda^\xi(\xi^\dagger \xi)^2,$$

$$V(\zeta) = \mu_\zeta^2(\zeta^\dagger \zeta) + \lambda^\zeta(\zeta^\dagger \zeta)^2,$$

$$V(\varrho) = \mu_\varrho^2(\varrho^\dagger \varrho) + \lambda^\varrho(\varrho^\dagger \varrho)^2,$$

and the interaction terms are,

$$\begin{aligned}
V(H, \chi) &= \lambda^{H\chi}(H^\dagger H)(\chi^\dagger \chi), \\
V(H, \Delta) &= \lambda^{H\Delta}(H^\dagger H) \text{Tr}(\Delta^\dagger \Delta), \\
V(H, \eta) &= \lambda^{H\eta}(H^\dagger H)(\eta^\dagger \eta), \\
V(H, \kappa) &= \lambda^{H\kappa}(H^\dagger H)(\kappa^\dagger \kappa), \\
V(H, \xi) &= \lambda^{H\xi}(H^\dagger H)(\xi^\dagger \xi), \\
V(H, \zeta) &= \lambda^{H\zeta}(H^\dagger H)(\zeta^\dagger \zeta), \\
V(H, \varrho) &= \lambda^{H\varrho}(H^\dagger H)(\varrho^\dagger \varrho), \\
V(\chi, \Delta) &= \lambda_1^{\chi\Delta}(\chi^\dagger \chi)(\Delta^\dagger \Delta) + \lambda_2^{\chi\Delta}(\chi^\dagger \chi)_{110}(\Delta^\dagger \Delta)_{120} + \lambda_3^{\chi\Delta}(\chi^\dagger \chi)_{101}(\Delta^\dagger \Delta)_{102} + \lambda_4^{\chi\Delta}(\chi^\dagger \chi)_{111}(\Delta^\dagger \Delta)_{122} + \lambda_5^{\chi\Delta}(\chi^\dagger \chi)_{121}(\Delta^\dagger \Delta)_{112} + \lambda_6^{\chi\Delta}(\chi^\dagger \chi)_{120}(\Delta^\dagger \Delta)_{110} + \lambda_7^{\chi\Delta}(\chi^\dagger \chi)_{102}(\Delta^\dagger \Delta)_{101} + \lambda_8^{\chi\Delta}(\chi^\dagger \chi)_{122}(\Delta^\dagger \Delta)_{111} + \lambda_9^{\chi\Delta}(\chi^\dagger \chi)_{112}(\Delta^\dagger \Delta)_{121}, \\
V(\chi, \eta) &= \lambda^{\chi\eta}(\chi^\dagger \chi)\eta^\dagger \eta, \\
V(\chi, \kappa) &= \lambda^{\chi\kappa}(\chi^\dagger \chi)\kappa^\dagger \kappa, \\
V(\chi, \xi) &= \lambda^{\chi\xi}(\chi^\dagger \chi)\xi^\dagger \xi, \\
V(\chi, \zeta) &= \lambda^{\chi\zeta}(\chi^\dagger \chi)\zeta^\dagger \zeta, \\
V(\chi, \varrho) &= \lambda^{\chi\varrho}(\chi^\dagger \chi)\varrho^\dagger \varrho, \\
V(\Delta, \eta) &= \lambda^{\eta\Delta} \text{Tr}(\Delta^\dagger \Delta)\eta^\dagger \eta, \\
V(\Delta, \kappa) &= \lambda^{\kappa\Delta} \text{Tr}(\Delta^\dagger \Delta)\kappa^\dagger \kappa, \\
V(\Delta, \xi) &= \lambda^{\xi\Delta} \text{Tr}(\Delta^\dagger \Delta)\xi^\dagger \xi, \\
V(\Delta, \zeta) &= \lambda^{\zeta\Delta} \text{Tr}(\Delta^\dagger \Delta)\zeta^\dagger \zeta, \\
V(\Delta, \varrho) &= \lambda^{\varrho\Delta} \text{Tr}(\Delta^\dagger \Delta)\varrho^\dagger \varrho, \\
V(\eta, \kappa) &= \lambda^{\eta\kappa}(\eta^\dagger \eta)\kappa^\dagger \kappa, \\
V(\eta, \xi) &= \lambda^{\eta\xi}\eta^\dagger \eta\xi^\dagger \xi, \\
V(\eta, \zeta) &= \lambda^{\eta\zeta}\eta^\dagger \eta\zeta^\dagger \zeta, \\
V(\eta, \varrho) &= \lambda^{\eta\varrho}\eta^\dagger \eta\varrho^\dagger \varrho, \\
V(\kappa, \xi) &= \lambda^{\kappa\xi}\kappa^\dagger \kappa\xi^\dagger \xi, \\
V(\kappa, \zeta) &= \lambda^{\kappa\zeta}\kappa^\dagger \kappa\zeta^\dagger \zeta, \\
V(\kappa, \varrho) &= \lambda^{\kappa\varrho}\kappa^\dagger \kappa\varrho^\dagger \varrho, \\
V(\xi, \zeta) &= \lambda^{\xi\zeta}(\xi^\dagger \xi)\zeta^\dagger \zeta, \\
V(\xi, \varrho) &= \lambda^{\xi\varrho}(\xi^\dagger \xi)\varrho^\dagger \varrho, \\
V(\zeta, \varrho) &= \lambda^{\zeta\varrho}(\zeta^\dagger \zeta)\varrho^\dagger \varrho, \\
V(H, \Delta, \chi) &= (H^T i\sigma_2 \Delta^T H \chi + h.c).
\end{aligned}$$

The term $V(H, \Delta, \chi)$ is important, as it is responsible for the vev of the Higgs triplet field, Δ . In models with discrete symmetry, it is common to have multiple coupling

constants in the scalar potential. This allows for the flexibility to choose appropriate vacuum alignments for the scalar fields. Without loss of generality, for the chosen vevs in the directions: $\langle \chi \rangle = v_\chi(1, 0, 0)$, $\langle H \rangle = v_h$, $\langle \Delta \rangle = v_\Delta(1, 1, 1)$, $\langle \eta \rangle = v_\eta$, $\langle \kappa \rangle = v_\kappa$, $\langle \xi \rangle = v_\xi$, $\langle \zeta \rangle = v_\zeta$ and $\langle \varrho \rangle = v_\varrho$, and using $\lambda_6^{x\Delta} = \lambda_2^{x\Delta}$, we have the following minimisation conditions of the scalar potential,

$$\begin{aligned}
\frac{\partial V}{\partial H} &= v_h(2v_h^2\lambda^H + 3\lambda^{H\Delta}v_\Delta^2 + v_\zeta^2\lambda^{H\zeta} + v_\eta^2\lambda^{H\eta} + v_\kappa^2\lambda^{H\kappa} + v_\xi^2\lambda^{H\xi} + v_\chi^2\lambda^{H\chi} + v_\varrho^2\lambda^{H\varrho} - \\
&\quad \mu_H^2 - 4v_\chi v_\Delta) = 0, \\
\frac{\partial V}{\partial v_{\chi_1}} &= v_h^2(v_\chi\lambda^{H\chi} - 2v_\Delta) + v_\chi(\mu_\chi^2 + 3\lambda_1^{x\Delta}v_\Delta^2 + 2v_\chi^2\lambda_1^x + 2v_\chi^2\lambda_2^x + v_\eta^2\lambda^{x\eta} + v_\kappa^2\lambda^{x\kappa} + v_\xi^2 \\
&\quad \lambda^{x\xi} + v_\zeta^2\lambda^{x\zeta} + v_\varrho^2\lambda^{x\varrho}) = 0, \\
\frac{\partial V}{\partial v_{\chi_2}} &= 3v_\chi\lambda_3^{x\Delta}v_\Delta^2 = 0, \\
\frac{\partial V}{\partial v_{\chi_3}} &= 3v_\chi\lambda_7^{x\Delta}v_\Delta^2 = 0, \\
\frac{\partial V}{\partial v_{\Delta_1}} &= v_h^2(\lambda^{H\Delta}v_\Delta - 2v_\chi) + v_\Delta(\mu_\Delta^2 + 6(\lambda_1^\Delta + \lambda_3^\Delta)v_\Delta^2 + v_\chi^2\lambda_1^{x\Delta} + 2v_\chi^2\lambda_2^{x\Delta} + v_\eta^2\lambda^{\Delta\eta} + v_\kappa^2 \\
&\quad \lambda^{\Delta\kappa} + v_\xi^2\lambda^{\Delta\xi} + v_\zeta^2\lambda^{\Delta\zeta} + v_\varrho^2\lambda^{\Delta\varrho}) = 0, \\
\frac{\partial V}{\partial v_{\Delta_2}} &= \frac{\partial V}{\partial v_{\Delta_3}} = v_\Delta(\mu_\Delta^2 + v_h^2\lambda^{H\Delta} + 6(\lambda_1^\Delta + \lambda_3^\Delta)v_\Delta^2 + v_\chi^2\lambda_1^{x\Delta} - v_\chi^2\lambda_2^{x\Delta} + v_\eta^2\lambda^{\Delta\eta} + v_\kappa^2\lambda^{\Delta\kappa} \\
&\quad + v_\xi^2\lambda^{\Delta\xi} + v_\zeta^2\lambda^{\Delta\zeta} + v_\varrho^2\lambda^{\Delta\varrho}) = 0, \\
\frac{\partial V}{\partial v_\eta} &= v_\eta(v_h^2\lambda^{H\eta} + \mu_\eta^2 + 3\lambda^{\Delta\eta}v_\Delta^2 + v_\chi^2\lambda^{x\eta} + 2v_\eta^2\lambda^\eta + v_\kappa^2\lambda^{\eta\kappa} + v_\varrho^2\lambda^{\eta\varrho} + v_\xi^2\lambda^{\eta\xi} + v_\zeta^2\lambda^{\eta\zeta}) \\
&= 0, \\
\frac{\partial V}{\partial v_\kappa} &= v_\kappa(v_h^2\lambda^{H\kappa} + \mu_\kappa^2 + 3\lambda^{\Delta\kappa}v_\Delta^2 + v_\chi^2\lambda^{x\kappa} + v_\eta^2\lambda^{\eta\kappa} + 2v_\kappa^2\lambda^\kappa + v_\varrho^2\lambda^{\kappa\varrho} + v_\xi^2\lambda^{\kappa\xi} + v_\zeta^2\lambda^{\kappa\zeta}) \\
&= 0, \\
\frac{\partial V}{\partial v_\xi} &= v_\xi(v_h^2\lambda^{H\xi} + 3\lambda^{\Delta\xi}v_\Delta^2 + v_\chi^2\lambda^{x\xi} + v_\eta^2\lambda^{\eta\xi} + v_\kappa^2\lambda^{\kappa\xi} + v_\varrho^2\lambda^{\xi\varrho} + 2v_\xi^2\lambda^\xi + v_\zeta^2\lambda^{\xi\zeta} + \mu_\xi^2) \\
&= 0, \\
\frac{\partial V}{\partial v_\zeta} &= v_\zeta(v_h^2\lambda^{H\zeta} + \mu_\zeta^2 + 3\lambda^{\Delta\zeta}v_\Delta^2 + v_\chi^2\lambda^{x\zeta} + v_\eta^2\lambda^{\eta\zeta} + v_\kappa^2\lambda^{\kappa\zeta} + v_\varrho^2\lambda^{\zeta\varrho} + v_\xi^2\lambda^{\xi\zeta} + 2v_\zeta^2\lambda^\zeta) \\
&= 0, \\
\frac{\partial V}{\partial v_\varrho} &= v_\varrho(v_h^2\lambda^{H\varrho} + \mu_\varrho^2 + 3\lambda^{\Delta\varrho}v_\Delta^2 + v_\chi^2\lambda^{x\varrho} + v_\eta^2\lambda^{\eta\varrho} + v_\kappa^2\lambda^{\kappa\varrho} + 2v_\varrho^2\lambda^\varrho + v_\xi^2\lambda^{\xi\varrho} + v_\zeta^2\lambda^{\zeta\varrho}) \\
&= 0.
\end{aligned}$$

Using the above minimisation equations, we further obtain:

$$\mu_H = (2v_h^2\lambda^H + 3\lambda^{H\Delta}v_\Delta^2 + v_\zeta^2\lambda^{H\zeta} + v_\eta^2\lambda^{H\eta} + v_\kappa^2\lambda^{H\kappa} + v_\xi^2\lambda^{H\xi} + v_\chi^2\lambda^{H\chi} + v_\rho^2\lambda^{H\rho} - 4v_\chi v_\Delta)^{1/2}, \quad (\text{A.9})$$

$$\mu_\chi = ((v_h^2(2v_\Delta - v_\chi\lambda^{H\chi}) - v_\chi(3\lambda_1^{x\Delta}v_\Delta^2 + 2v_\chi^2\lambda_1^x + 2v_\chi^2\lambda_2^x + v_\eta^2\lambda^{x\eta} + v_\kappa^2\lambda^{x\kappa} + v_\rho^2\lambda^{x\rho} + v_\xi^2\lambda^{x\xi} + v_\zeta^2\lambda^{x\zeta}))/v_\chi)^{1/2}, \quad (\text{A.10})$$

$$\mu_\Delta = (-v_\chi^2v_h^2\lambda^{H\Delta} - \frac{8}{3}(\lambda_1^\Delta + \lambda_3^\Delta)v_h^4\lambda_2^{-2x\Delta} + v_\chi^4\lambda_2^{x\Delta} - v_\chi^2(v_\chi^2\lambda_1^{x\Delta} + v_\eta^2\lambda^{\Delta\eta} + v_\kappa^2\lambda^{\Delta\kappa} + v_\rho^2\lambda^{\Delta\rho} + v_\xi^2\lambda^{\Delta\xi} + v_\zeta^2\lambda^{\Delta\zeta}))^{1/2}/v_\chi, \quad (\text{A.11})$$

$$v_\Delta = \frac{2v_h^2}{3\lambda_2^{x\Delta}v_\chi}, \quad (\text{A.12})$$

$$\lambda_3^{x\Delta} = \lambda_7^{x\Delta} = 0. \quad (\text{A.13})$$